JJMIE

Volume 9 Number 3, June.2015
ISSN 1995-6665
Pages 209 - 216

Jordan Journal of Mechanical and Industrial Engineering

Investigation of Sweep Angle Effects on a Submarine Hydrodynamic Drag Using Computational Fluid Dynamics

Mohammad Hadipour, Ebrahim Goshtasbi rad*

Department of Aerospace and energy, School of mechanical engineering Shiraz University, Shiraz, Iran

Received 11 Jan 2015 *Accepted 1 June 2015*

Abstract

In the present paper, the effects of the increase in surfaces backward sweep angle of horizontal tail and the hydrofoil of a typical submarine on its hydrodynamic drag are investigated with Computational Fluid Dynamics (CFD). Results show that with the increase in the horizontal tail backward sweep angle about 50° in constant surface area, hydrodynamic drag can reduce 6% than zero backward sweep angle condition. This value is equal to 44 N reductions in hydrodynamic drag force and 180 watt of consumption power in 4 m/s speeds of this submarine. Also, with increasing 60° of this submarine hydrofoil backward sweep angle, the constant hydrofoil volume can reduce 14% from hydrodynamic drag rather than zero hydrofoil backward sweep angle. This hydrodynamic drag reduction of this typical submarine in cruising speed (4 m/s) is equal to 97 N force, saving 388 watt of the consumption power. In general, the 50° of horizontal tail backward sweep angle and 60° of hydrofoil backward sweep angle can reduce 19% of hydrodynamic drag rather than zero tail and hydrofoil backward sweep angles. These amounts of drag reduction and power saving in this typical submarine can increase the range and the endurance.

Keywords: *CFD, Hydrodynamic Drag, Sweep Angle, Drag Reduction*.

1. Introduction

One of the most important parameters in designing vehicles that move in fluids, such as aircrafts or submarines, is the proper aerodynamic or hydrodynamic design. In general, suitable aerodynamic or hydrodynamic design is increasing in lift coefficient and moves toward the minimum value of drag coefficient [1]; but in ships and submarines, the main subject is hydrodynamic drag force reduction regardless of lift coefficient [2-5]. In the present paper, an investigation of the drag reduction is done on a special type of small scale unmanned submarine. The main purpose is to reduce the hydrodynamic drag using the implementation of proper geometrical shape changes, whereas the hydrofoil volume and the horizontal tail surface area remain fixed (hydrofoil surface area and horizontal tail volume are set as fixed parameters) because the main systems of this unmanned submarine and water tank located in the hydrofoil and its volume reduction can cause problems in necessary systems packaging. Figures 1 and 2 show the shape of this unmanned submarine and its dimensions.

Nature has always been the best inspiration for engineers and designers in all industrial fields, especially in aerospace and marine industries [2]. For drag reduction in this vehicle, the idea is to apply a backward sweep angle in submarine hydrofoil and horizontal tail, like fish bodies. This idea, proposed by the present authors, is unique and does not in any other report. Implementation of backward and forward sweep angles in near sonic and supersonic aircraft wings can reduce wings wave drag due to the reduction in the normal velocity component on wing leading edge and can decrease the local Mach number (increase in critical Mach number) [6]. The present study is part of a study on a multi-mission vehicle [7], concentrated on the investigation of the backward sweep angle effects of hydrofoil and horizontal tail in incompressible subsonic (very low speed) regime and dense environment of water. At first, with fixed hydrofoil shape (zero sweep angle), horizontal tail sweep angle changes from 0° to 50°. Figure 3 illustrates the variation in the horizontal tail sweep angle. Tail airfoil and main hydrofoil have a standard section of NACA0012 and NACA0019, respectively.

* Corresponding author. e-mail: goshtasb@shirazu.ac.ir.

  - Volume 9, Number 3 (ISSN 1995-6665)

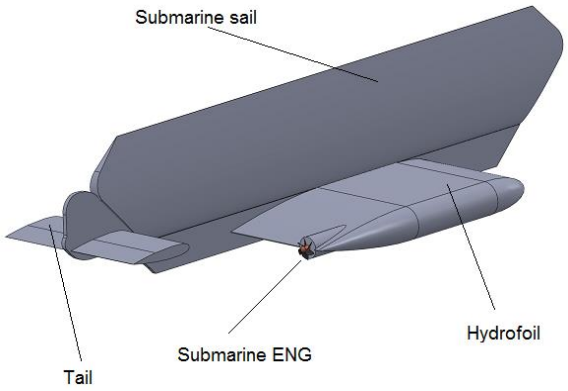

Figure 1. Components of studying submarine in basic shape (zero hydrofoil and horizontal tail sweep angle)

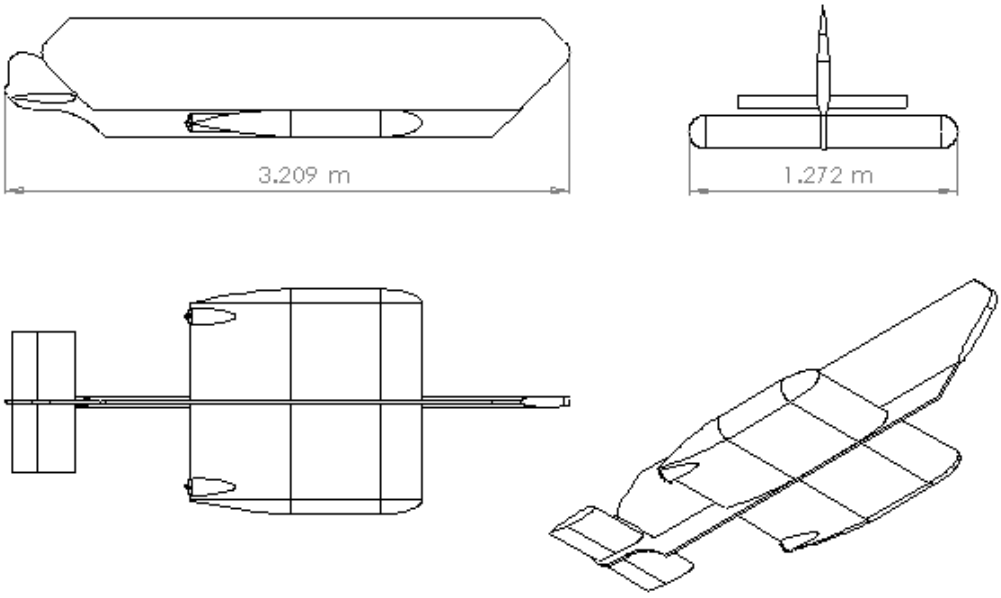

Figure 2. Standard views of studying submarine in basic shape (zero hydrofoil and horizontal tail sweep angle)

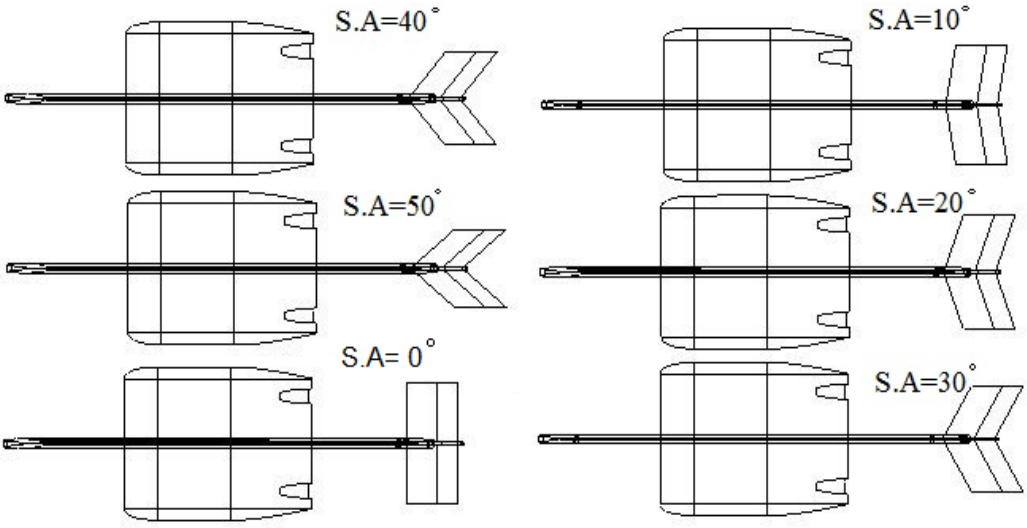

Figure 3. Submarine with fixed hydrofoil and swept horizontal tail that change from $0°$ to $50°$

In the first step, the hydrofoil sweep angle is zero (constant) and the tail sweep angle increases from 0° to 50°; then, in the next step, with a constant horizontal tail sweep angle, the effects of applying hydrofoil sweep angle, that changes from 0° to 60° degrees, is investigated. Figure 4 illustrates how the hydrofoil sweep angle changes with the fixed (50°) horizontal tail sweep angle:

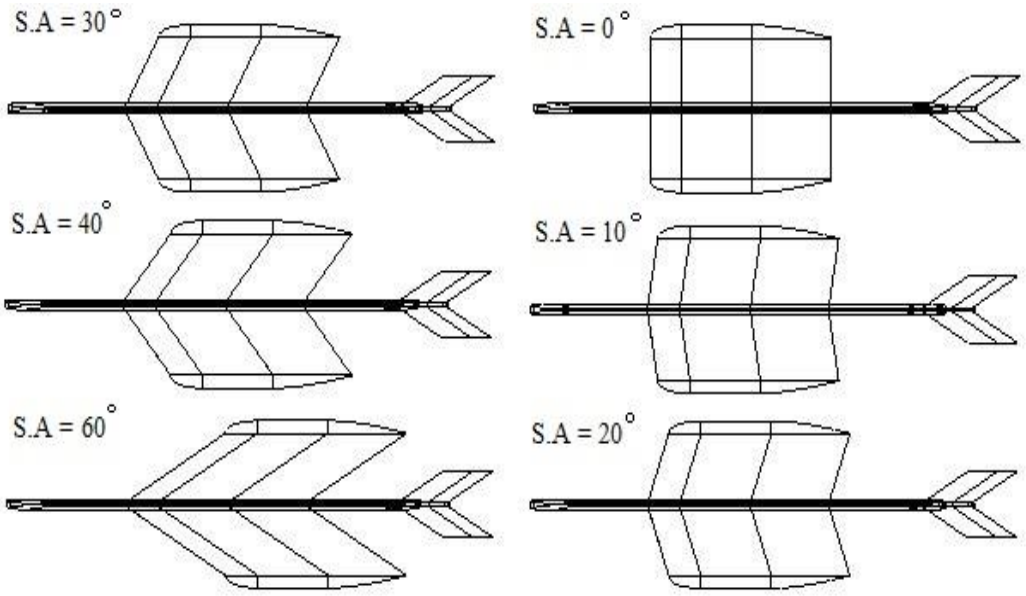

Figure 4. Submarine with fixed horizontal tail and swept hydrofoil that change from 0° to 60°

When the sweep angles of the hydrofoil and the tail are changed (in Mechanical Design Software), the orthogonal span is also changed. Therefore, authors decided to maintain the volume of the hydrofoil and the tail surface as a fixed parameter because of their missions and only to show the infuence of the sweep angles on drag reduction. Figure 5 shows the elongation of span to fix the hydrofoil volume:

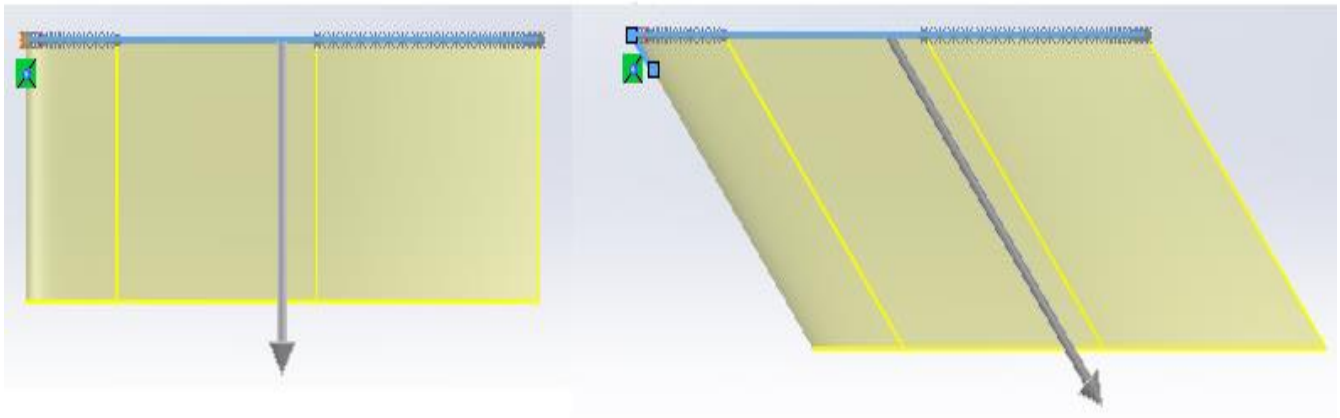

Figure 5. Increase extrude length of hydrofoil in non zero sweep angles to maintain constant hydrofoil volume

The present study is built of the bases that submarines usually move with zero angle of attack and that 4m/s (7.8 knots) is the maximum cruise speed of the proposed submarine.

2. Numerical Approach

The CFD method is convenient and time saving. To ensure reliable results and since experimental data were not available for this submarine, ANSYS Fluent and ANSYS CFX software were used. Different computational grids were generated with various quality and characteristics to ensure the independence of the model from computational grid. In addition, mesh density control was applied in order to save computational power and time by setting coarse grids at the boundaries of the domain and fine grids near area of interests and where the geometries are more complex. Mesh density near the walls and at the boundary layer can properly predict a viscous force on submarine surfaces. The Computational domain in both CFX and FLUENT has the same extent and size but has different boundary layer mesh due to differences in these solvers (Table.1).

Table 1. Comparison of boundary layer mesh characteristics in CFX and FLUENT

CFD Software	Transition Ratio	Maximum Layer	Growth Rate 3	Collision Avoidance
FUENT	0.272	5	1.2	Layer Compression
CFX	0.77	5	1.2	Stair Stepping

In addition, to avoid generating any highly skew mesh, mesh control is also needed to ensure that the transition from fine to coarse mesh is smooth. After the implementation of the computational grid and the domain study methods, mesh refinements are done in five steps. The total number of cells in the chosen computational grid is approximately 4.5 million. This is thought, by the authors, to be rough to give accurate results but proper to capture the characteristics of the flow properties; see Figure 6.

For the computational domain, the inflow was placed 6*c* upstream of the submarine nose, the outflow 15*c* downstream and 6*c* in height (c is hydrofoil mean chord), as shown in Figure 7. The side boundary was placed 6*c* away from hydrofoil tip. The y+ value at the wall is around 200, which is suitable for wall function applied in numerical simulation. A velocity inlet boundary condition prescribed a uniform velocity of 4m/s. At the outflow boundary, a pressure outlet boundary condition specified a gauge pressure of zero. A slip boundary condition (symmetry) was specified on the top and side far boundaries. A no-slip boundary condition was specified on the submarine surfaces. Domain is mono-phase and water has a constant density of 998.2 kg/m^3 and its viscosity set to 0.001003 kg/ms.

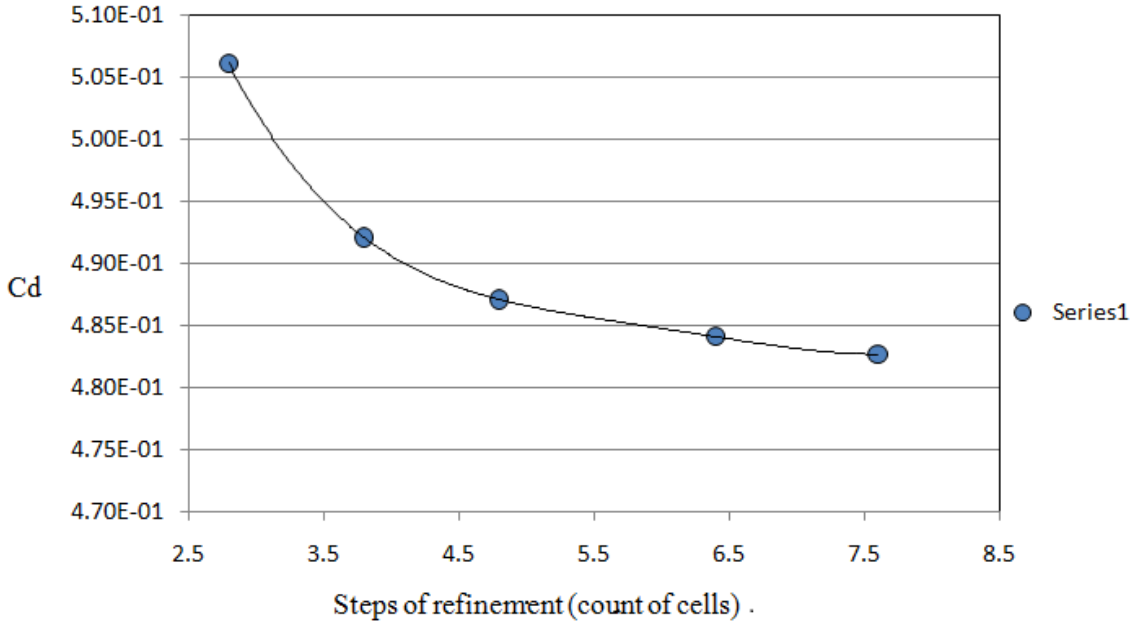

Figure 6. Hydrodynamic drag coefficient versus number of meshes(million grids).

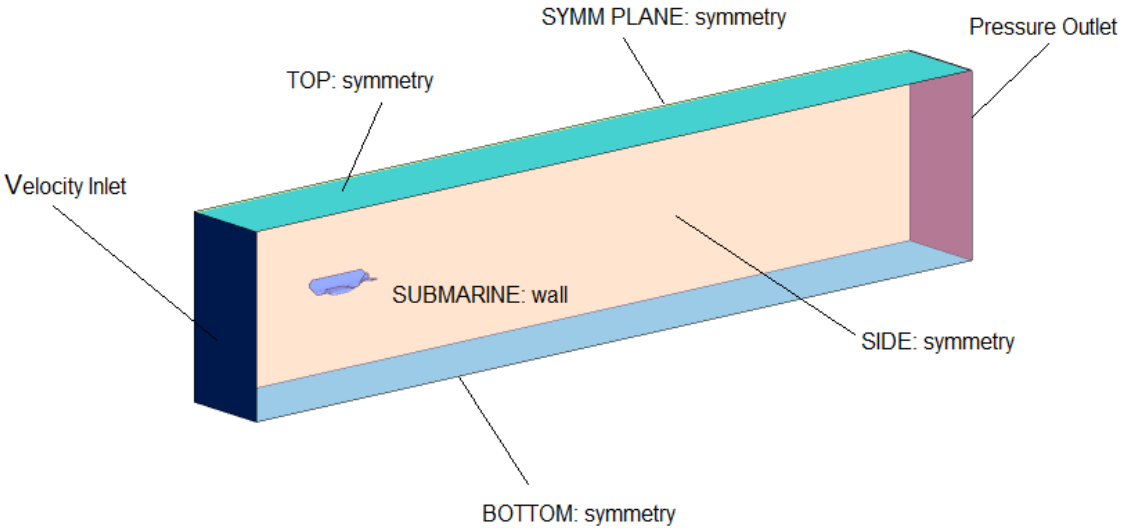

Figure 7. Applied boundary conditions on computational domain

Unstructured boundary layer mesh was used for simulations due to its good adaption ability to complex geometries and its reliability. Unstructured boundary layer mesh was generated in ANSYS Mesher and CFD analysis was carried out using FLUENT and ANSYS CFX commercial codes. Results show good agreements between FLUENT and CFX data that confirmed each other. Various turbulent models were used in both software but the best results in FLUENT was realizable *k*-ε model and in CFX was standard *k*-ε model.

2.1. Governing Equations

In the present study, flow regime is simulated by solving the incompressible Reynolds-averaged Navier-Stokes equations with the realizable $k-\varepsilon$ turbulence model in FUENT at the Reynolds number of 12.72×10^9 (based on the length of submarine).

The governing equations are written as:

$$\frac{\partial U_i}{\partial x_i} = 0 \tag{1}$$

$$\frac{\partial U_i}{\partial x_i} + \frac{\partial (U_i U_J)}{\partial x_j} = -\frac{1}{\rho}\frac{\partial p}{\partial x_i} + v\frac{\partial^2 U_i}{\partial x_j \partial x_j} + \frac{\partial}{\partial x_j}(\overline{-\acute{u}_i \acute{u}_j}) \tag{2}$$

where $(\overline{-\acute{u}_i \acute{u}_j})$ is the Reynolds stress term.

The transport equations of *k* and ε are written as:

$$\frac{\partial}{\partial t}(\rho k) + \frac{\partial (\rho k u_j)}{\partial x_j} = \frac{\partial}{\partial x_j}\left[\left(\mu + \frac{\mu_t}{\sigma_k}\right)\frac{\partial k}{\partial x_j}\right] + G_k + G_b - \rho\varepsilon - Y_M + S_k \tag{3}$$

$$\frac{\partial}{\partial t}(\rho\varepsilon) + \frac{\partial (\rho\varepsilon u_j)}{\partial x_j} = \frac{\partial}{\partial x_j}\left[\left(\mu + \frac{\mu_t}{\sigma_\varepsilon}\right)\frac{\partial \varepsilon}{\partial x_j}\right] + \rho C_1 S\varepsilon - \rho C_2 \frac{\varepsilon^2}{k + \sqrt{v\varepsilon}} + C_{1\varepsilon}\frac{\varepsilon}{k}C_{13\varepsilon}G_b + S_\varepsilon \tag{4}$$

The realizable κ-ε model is a more advanced version of a two-equation turbulence model. This turbulence model was extensively validated and well behaved for a wide range of flows, including rotating homogeneous shear flows, free flows including jets and mixing layers, channel and boundary layer flows, and separated flows [8, 9]. The incompressible Navier-Stokes equations (eq. (1) and eq. (2)) are solved by the SIMPLE [10] algorithm with a second-order upwind scheme applied to the convection terms. Also, in the operating condition panel, the operating pressure was set at 1 atmosphere and gravity was activated. Near wall treatment was set as a scalable wall function that is a new method and has a better convergence in two solvers. A default set of under-relaxation factor was suitable for a solver convergence.

To ensure the proper convergence of the solutions, a study is made on the tolerance value needed for the convergence criteria. Since the drag is the most important parameter needed, the solutions of this parameter is observed with a different tolerance value. When the fluctuation of the drag is sufficiently small in the next successive steps of iterations, the solutions are said to have converged sufficiently.

3. Results

In the first step of simulations, results show that the increase in the horizontal tail sweep angle with constant zero hydrofoil backward sweep cause hydrodynamic drag reduces about 6% in 50° tail backward sweep angle. This reduction of hydrodynamic drag in 4m/s speeds of this submarine is equal to 44 N; therefore, the consumption power decreases about 180 watt; see Figure 8.

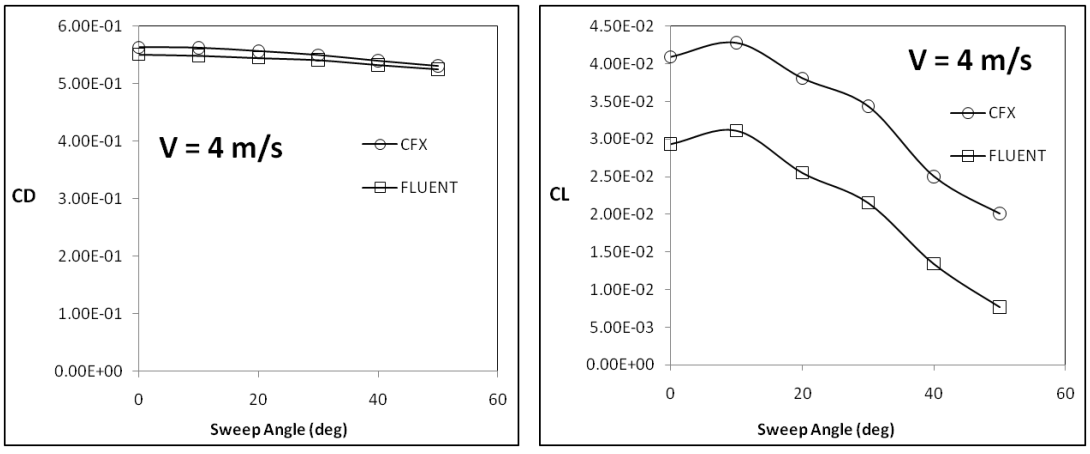

Figure 8. Hydrodynamic drag and lift coefficient versus horizontal tail sweep angle (constant zero hydrofoil sweep angle)

In the next step, hydrofoil sweep angle that has a larger cross section and a wetted area and subsequent has more contribution in the hydrodynamic drag graduate from 0° to 60° but the horizontal sweep angle remains 50° fixed.

Figure 9 illustrates how the increase in the hydrofoil sweep angle decreases the hydrodynamic drag. CFX and FLUENT results are in agreement with each other.

Figure 9 shows that in 4m/s of the submarine speed, with 60° increasing in hydrofoil sweep angle, hydrodynamic drag coefficient decreases about 14% rather than zero hydrofoil sweep angle. This amount of drag reduction is equal to 97 N and 388 watt of consumption power in maximum cruising speed causing an increase in the submarine range and endurance.

Figures 10 and 11 illustrate velocity contours behind the submarine in parallel section planes and Figures 12 and 13 show the velocity contours in longitudes plan (top view) in two conditions consisting of hydrofoils zero and 60° sweep angles. Contours show how the hydrofoil sweep angle desirably alters the pressure and velocity contribution to decrease the wake and hydrodynamic drag force. Therefore, the overall drag reduction without any reduction in the hydrofoil volume and the horizontal tail surface area, as shown in Figure 14, reaches about 19% rather than zero sweep angle condition of tail and hydrofoil. This hydrodynamic drag is equal to 141 N and 564 watt of consumption power in cruise (4m/s) speed.

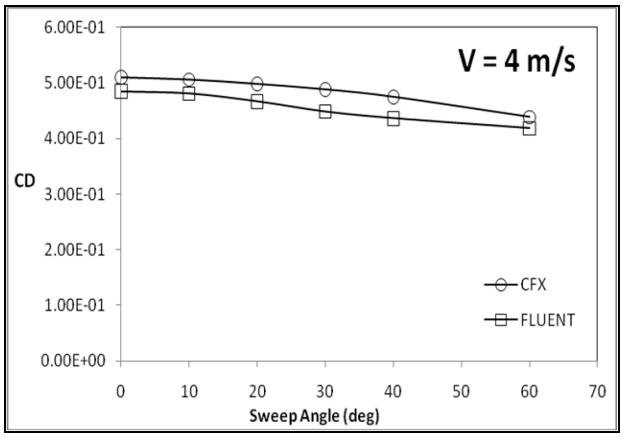

Figure 9. Hydrodynamic drag coefficient versus hydrofoil sweep angle (constant 50° horizontal tail sweep angle)

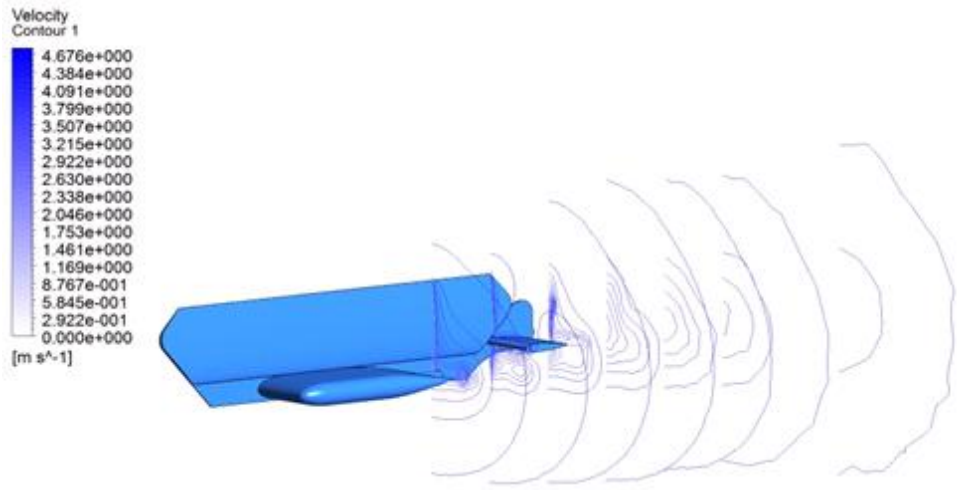

Figure 10. Velocity contours in parallel section planes with zero hydrofoil and tail sweep angle

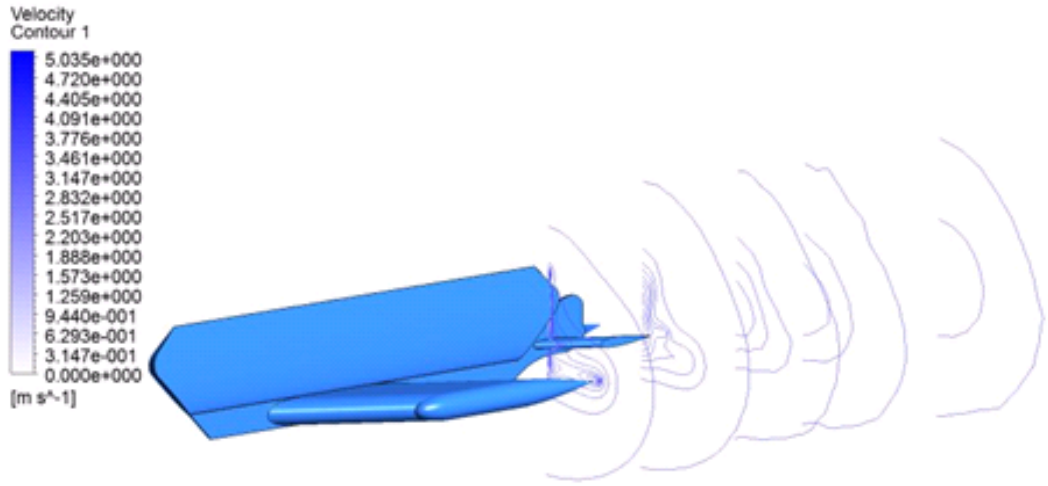

Figure 11. Velocity contours in parallel section planes with 60° hydrofoil and 50° tail sweep angle

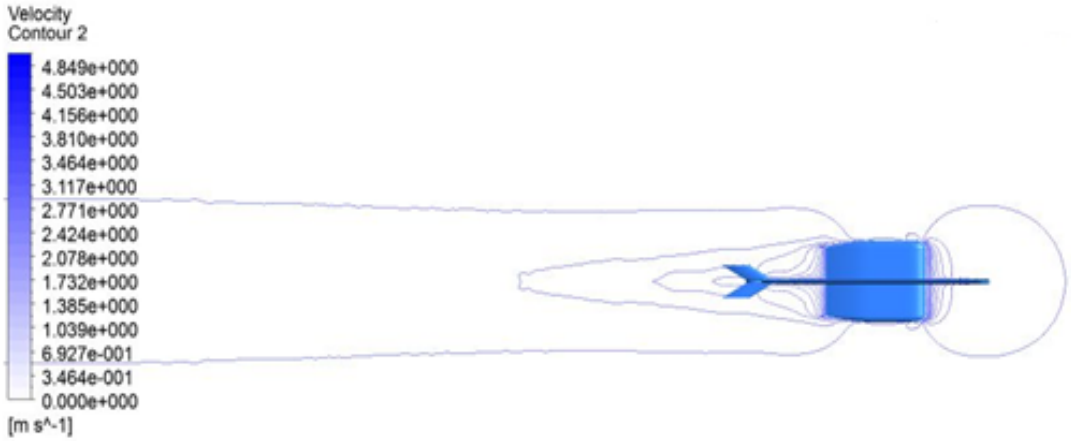

Figure 12. Velocity contours in longitude plane (top view) with zero hydrofoil and 50° tail sweep angle

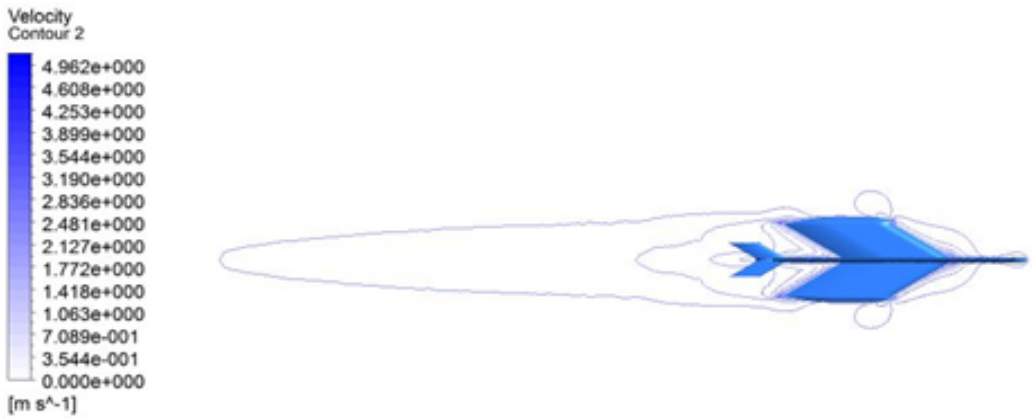

Figure 13. Velocity contours in longitude plane (top view) with 60° hydrofoil and 50° tail sweep angle

4. Conclusion

Results show that the implementation of backward sweep angle on control surfaces and hydrofoil (main body) of small scale submarine with a new design that has a non-cylindrical shape and shapes like as airplanes unlike classic submarine cylindrical body, same as wave drag reduction in supersonic aircrafts flight can be effective in reducing the hydrodynamic drag in low speed dense fluid regime like water.

It's clear that applying a backward sweep angle on control surfaces and hydrofoil with a reduction in the maximum normal to chord cross section in constant volume even in more surface area of hydrofoil results in significant changes in pressure contribution in the front of the hydrofoil and a reduction in the wake area behind of the submarine. Wake zone reduction due to sweep of hydrofoil can increase the secrecy of this submarine that is an important parameter in such a vehicle design. Therefore, with applying a backward sweep angle on this submarine surface, and similar cases, can reduce the engine consumption power and save fuel and cost.

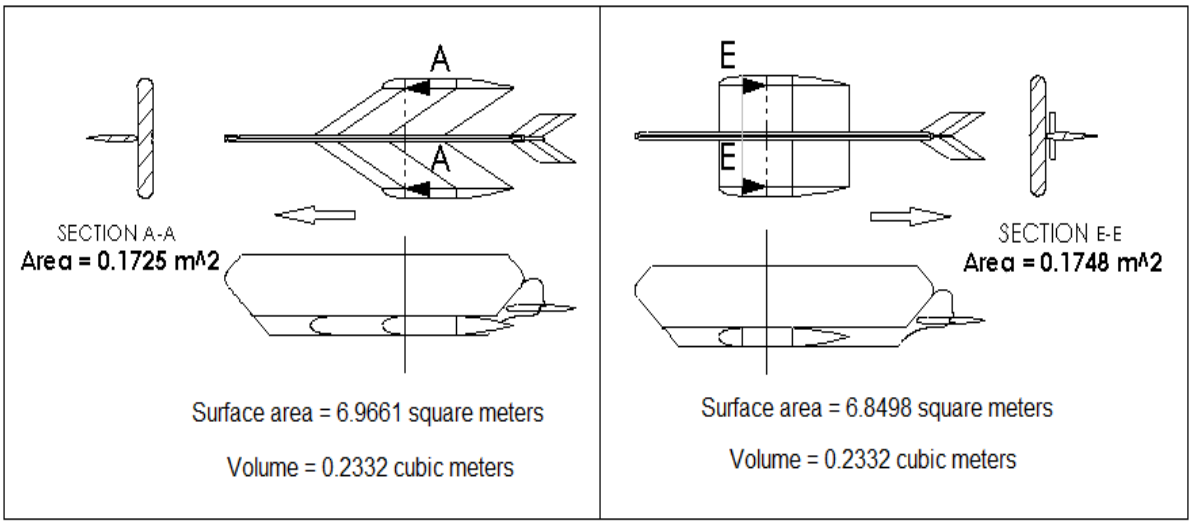

Figure14. comparing of wetted area, overall volume and maximum cross section area of submarine in zero and 60° hydrofoil sweep angles

References

[1] Hossain, P.R. Arora, A. Rahman, A.A. Jaafar and A.K.M. Parves Iqbal, "Analysis of longitudinal aerodynamic characteristics of an aircraft model with and without winglet". Jordan Journal of Mechanical and Industrial Engineering Vol. 2 (2008), No. 3, pp 143 - 150

[2] F.E. Fish, "Imaginative solutions by marine organisms for drag reduction". Department of biology, West Chester University, West Chester, PA 19383 USA, (2012), www.researchgate.net

[3] Zobeiri, "Effect of hydrofoil trailing edge geometry on the wake dynamics". PhD. Theses No. 5218. Ecole Polytechnique Federal de Laussanne, (2012)

[4] M.H. Djavareshkian, A. Esmaeili and A. Parsania, "Numerical simulation of smart hydrofoil in marine systems". Ocean Engineering 73 (2013) pp 16-24

[5] Ashrafi, M. Ketabdari and H. Ghassemi, "Numerical study on improvement of hydrofoil performance using vortex generators". IJE Transaction B: Application, Vol. 28 (2015) No.2 pp 305-313

[6] Roskam, J., and Edward Lan C.T. "Airplane aerodynamics and performance". Kansas, Lawrence, DARcorporation, (1997), pp. 112-114

[7] M. Hadipour and E. Goshtasbi Rad, "Investigation and comparing between two air propulsion systems used in a multipurpose vehicle using computational fluid dynamics" Journal of Science and Engineering, Vol. 5 (2014), No. 1, pp. 11-23

[8] T.H. Shih, W.W. Liou, A. Shabbir, and Z. Yang, "A new *k*-*ε* Eddy-viscosity model for high Reynolds number turbulent flows - model development and validation" Computers Fluids, Vol. 24 (1995) ,No. 3: pp. 227-238.

[9] M.P. Bulat and P.V. Bulat, "Comparison of turbulence models in the calculation of supersonic separated flows". World Applied Science Jour. 27 (2013), Issue 10, pp 1263-1266.

[10] Patankar, S.V., Numerical heat transfer and fluid flow, McGraw-Hill, 1980, pp.126-130.